The Role of Rapid Changes in Weather on Phytoplankton Spring Bloom Dynamics Captured by an Autonomous Uncrewed Surface Vehicle

G. M. Fragoso[1,2]†, A. Dallolio[3], S. Grant[1,2], J. L. Garrett[3], I. Ellingsen[4], G. Johnsen[1,2,5] and T. A. Johansen[2,3]

[1]Trondheim Biological Station, Department of Biology, Norwegian University of Science and Technology (NTNU), Trondheim, Norway.

[2]Centre of Autonomous Marine Operations and Systems (AMOS), NTNU, Trondheim, Norway.

[3]Department of Engineering Cybernetics, NTNU, Trondheim, Norway.

[4]SINTEF Ocean, Dept. Env. & New resources, Trondheim, Norway.

[5]University Centre in Svalbard (UNIS), Longyearbyen, Norway.

Corresponding author: Glaucia M. Fragoso (glaucia.m.fragoso@ntnu.no)

† Bynesveien 46, 7018, Trondheim, Norway.

Key Points:

- The spring bloom in coastal high latitudinal regions consisted of multiple peaks associated with gain and loss processes.
- Relaxation of strong winds and clear skies for 7-10 days in spring allowed phytoplankton accumulation and bloom development.
- Episodic strong winds interluded spring bloom development after a period of calm, sunny weather.

Abstract

The spring phytoplankton bloom plays a major role in pelagic ecosystems; however, its dynamics is overlooked due to insufficient, highly-resolved observational data. Here we investigate the start, peak and decline of a two-week phytoplankton spring bloom in Frohavet, located at the coast of mid-Norway. We used observations from an uncrewed surface vehicle (USV) combined with buoy measurements, satellite images, discrete water sampling and modelling approaches. The spring bloom (March-June 2022) consisted of multiple peaks (up to 5 mg m^{-3}), with a long peak in April, coincident with the period when the USV captured the temporal and spatial dynamics of the bloom. Short-term (5 days) episode of calm weather in the spring, such as clear skies and consistent low wind speed (< 7 m s^{-1}) shoaled the mixed layer depth (< 15 m), after strong wind speed (average wind speed up to 20 m s^{-1} in March) and mixing events in winter. These rapid changes in the environment promoted the rapid development of the spring bloom - from 1 to 5 mg m^{-3} in 5 days. Likewise, the collapse of the bloom was rather quick, 1-2 days and coincides with low nitrate values and rapid increase in wind speed (> 10 m s^{-1}), suggesting strong influence of the environment on phytoplankton dynamics during early stages of the spring bloom. Understanding the dynamics of the spring bloom is crucial for the management of marine resources. Integration of distinct observational platforms has the potential to unveil the environmental factors underlying phytoplankton bloom dynamics.

Plain Language Summary

The phytoplankton spring bloom is an important recurrent phenomenon because it provides food for the marine food web and regulates the climate. Although previous studies were focused on the initiation of the spring bloom, its dynamics, meaning, rapid changes in formation and decline, are usually not observed in detail. Here we used a combination of a technological (marine sensors and robots) and traditional methods (water collection, laboratorial and microscopic analyses) to observe the spatial and temporal variation of the spring bloom in a biological hotspot of the coast of mid-Norway. Small windows of 'good weather', where few days of sunny, clear skies and weak winds in the midst of 'stormy spring' promoted the rapid development of the spring bloom dominated by the diatom *Skeletonema*. The bloom collapsed after the wind speed got high again, suggesting the strong influence of environmental conditions in the spring bloom. Here we demonstrated that the use of multiple ocean observation platforms is crucial to understand, in detail, the processes controlling the spring phytoplankton bloom.

Index terms
4855 Phytoplankton 4894 Instruments, sensors, and techniques 4271 Physical and chemical properties of seawater

Keywords: phytoplankton dynamics, environmental controls, phytoplankton spring bloom, non-photochemical quenching, uncrewed surface vehicles.

1 Introduction

The spring phytoplankton bloom is a key event in the annual cycle of phytoplankton abundance in high latitudinal seas (Chiswell et al., 2014; Rumyantseva et al., 2019). As a recurrent seasonal phenomenon, the spring bloom plays a major role in pelagic ecosystems, contributing to carbon export and sequestration, oxygen production and energy flow for higher trophic levels (Alkire et al., 2014). Phytoplankton spring bloom are also sentinels of climate change, where alterations in intensity and phenology have been observed (Edwards & Richardson, 2004), with predictions of a continuous shift by the end of the century (Henson et al., 2018; Yamaguchi et al., 2022)

In simple terms, phytoplankton spring blooms consist of positive biomass accumulation rate (r) over a period of time, where growth (μ, e.g. cellular division) surpasses loss processes (l, e.g., grazing and sinking rates, viral lysis) ($r = \mu - l$, $r > 0$). While there is a scientific consensus that spring blooms consist of accumulation of phytoplankton, the processes that determine their start and the net balance between μ and l, are still on debate (Mojica et al., 2021). Moreover, there is also a debate of what constitute a bloom, whether accumulation is explosive (rapidly increase in r) or steadily increasing over time (Mignot et al., 2018). Historically, $r > 0$ in spring was viewed as a bottom-up process, where l remained unchanged and μ increased rapidly as light becomes a non-limiting factor with shoaling of the mixed layer (Sverdrup, 1953). Recently, this hypothesis has been contested, where low l due to low grazing rates as a consequence of low encounter rates of phytoplankton and zooplankton, rather than a fast change in μ in spring, would account for slow $r > 0$ in winter (Behrenfeld, 2010; Behrenfeld et al., 2013; Behrenfeld & Boss, 2014). These authors also suggested that tight recoupling between grazers and phytoplankton occur when the mixed layer start to become shallow, with a slight lag (1 day) in time, where l,

the deterministic factor for $r > 0$, would eventually catch up with μ after an early stock of phytoplankton biomass in winter (Behrenfeld & Boss, 2014).

The debate around spring bloom is mostly focused on their initial stage, although, in reality, these such blooms are quite dynamic in high latitudinal and polar seas (Behrenfeld et al., 2017). This means that weather changes (e.g. cloud cover, wind speed), particularly in spring, are rather fast (< 1 day), where the volatile nature of these blooms consists of multiple peaks with rapid formation and collapse over the course of few days or weeks. Thus, many studies ignore the influence of 'small windows of good weather', where few days of sunny, clear skies and weak winds during a 'stormy spring' might have a huge impact on phytoplankton dynamics.

Central to this problem is the lack of sufficient, highly-resolved observational data, particularly for regions that are highly dynamic and complex. For many years, spring blooms have been studied using satellites, which close progression of blooms are missed due to cloud cover often occurring in high latitudinal seas (Behrenfeld, 2010). Discrete water and net sampling over a long-term time series provides detailed information of plankton species (González-Gil et al., 2022); however, microscopic analyses are time-consuming and, in many times, not highly resolved in space and time. Fixed platforms, including buoys, can provide high temporal resolution (< 1h), however, spatial patchiness is often be missed (Son et al., 2014). Mobile platforms, including profiling floats (Boss & Behrenfeld, 2010; Mignot et al., 2018) and gliders (Rumyantseva et al., 2019) are suitable, but only for deep, open waters (> 200 m) due to the potential collision to a shallow seafloor. For coastal regions, with shallow and irregular bathymetry, autonomous uncrewed surface vehicles (USV) can offer an affordable, flexible solution for studying phytoplankton spring bloom progression, although observations comprise only surface waters (Dallolio et al., 2021; Scott et al., 2020). Modelling approaches can offer

complementary information regarding areas not covered by satellites and USVs and can also provide the vertical structure of the water column. An "observational pyramid" for ocean systems, which combines the integration of in-situ autonomous platforms, fixed buoys, satellite imagery and modelling approaches with discrete net and water sampling have the capacity to unveil the dynamics of a phytoplankton spring bloom in a coastal, productive hot-spots (Fragoso et al., 2022; Williamson et al., 2023).

In-situ chlorophyll *a* fluorescence (*FChla*) measurements derived from sensors attached to autonomous or fixed platforms have been historically used as a proxy of phytoplankton biomass in studies of bloom dynamics (Roesler et al., 2017). However, *FChla* measurements are only useful when they reflect the true concentration of chlorophyll *a* [*Chla*] in the water. Systematic errors, such as biofouling and non-photochemical quenching (*NPQ*) influence the fluorescence signal to intracellular *Chla* pigment ratios, offering biased measurements (Carberry et al., 2019; Johnsen et al., 2018; Scott et al., 2020). *NPQ* is a physiological response of live cells to high light (usually observed in surface waters at daytime), where the excess of energy is converted to heat, reducing the *FChla* signal (Huot & Babin, 2010). Thus, it is crucial that, for surface *FChla* measurements derived from USVs, values are corrected for *NPQ*, particularly during spring and summer.

Here, we use an USV equipped with environmental and weather sensors (fluorometer, CTD, oxygen optode and weather station) to investigate the dynamics (start, peak and decline) of a 2-week phytoplankton spring bloom in Frohavet, a coastal Norwegian biological hotspot. To complement the USV data (resolved to 1 min binned), a combination of other observational methods, including a fixed mooring buoy, satellite images, discrete water sampling and modelling approaches were included. For *FChla* from the USV, we provide a solution for *NPQ*

for daily changes and investigate the biophysical controls of the bloom. Discrete water samples for nutrient concentrations and phytoplankton abundances, in addition to *FChla* measurements from a moored buoy, were collected from a fixed station ~25 km away from the trajectory of the USV AutoNaut. Integration of distinct observational platforms, such as autonomous vehicles, fixed buoys, discrete water sampling and modelling approaches has the potential to unveil the environmental factors underlying phytoplankton bloom dynamics.

2 Materials and Methods

2.1 Study area

Frohavet is a wide, open stretch of sea surrounded by a large cluster of small islands on the coast of Trøndelag, mid-Norway (Fig. 1). This region sustains high levels of primary production and biological diversity and is a popular site for aquaculture activities. Frohavet is highly productive because of the Norwegian Atlantic Water (NAW), which brings nutrient-rich Atlantic Water (AW) along the shelf break. This water mass is located below the Norwegian Coastal Current (NCC), which becomes thicker as freshwater input increases from spring to summer (Fragoso et al., 2019). The NAW often reaches the surface through coastal upwelling and internal waves (Fragoso et al., 2019). Diatoms are known to be the predominant phytoplankton of the spring bloom (Fragoso et al 2021, Thu et al 2021), however, dinoflagellates often to co-occur. Diatoms blooms sustains high zooplankton (particularly copepods) abundance predominantly found in this region (Fragoso et al., 2019).

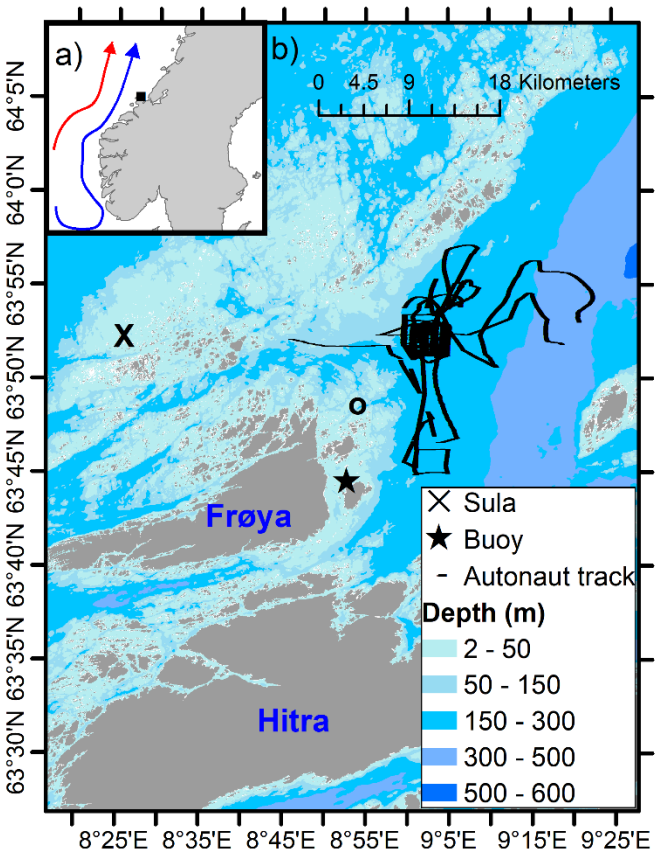

Figure 1- Study site in the coast of mid-Norway. a) Scheme showing the main currents flowing northwards – the Norwegian Coastal Current (blue) and the Norwegian Atlantic Current (red). b) Map of Frohavet region showing the islands of Frøya and Hitra, in addition to the weather station in Sula Island (cross symbol), the fixed buoy station near Frøya (star symbol) and the site where mixed layer depth was modelled by SINMOD (circle symbol).

2.2 Buoy and water sampling

To monitor the start and development of the bloom in the region of Frohavet, a C3 submersible fluorometer sensor (Turner Designs, USA) was attached into a buoy located about 2 km east of the coast of Frøya Island (Fig. 1) and placed at 4 m depth (Fig. 1). This sensor collected temperature (°C), *FChla* (calibrated later to concentration in mg m^{-3}) and turbidity (Relative Fluorescence Unit - calibrated later to Formazin Turbidity Unit (FTU)) every 10 min from mid-February to mid-June. Hourly wind speed (m s^{-1}) data (from February until mid-June) from Sula

meteorological station (located in the western part of Frohavet) were collected from the Norwegian Weather Service Center (https://seklima.met.no/). A HOBO pendant temperature and light logger (HOBO, USA) was placed at the top of the buoy to measure light intensity in air (measurement in lux at every 30 min from February until June). Values were integrated daily and converted to photosynthetic active radiance (µmol photons m^{-2} s^{-1}) by using a conversion factor: 1 klux (kilolux)= 14-18 µmol photons m^{-2} s^{-1} (Sakshaug et al., 2009).

Discrete water sampling for nitrate and *in vitro* chlorophyll concentrations ([$Chla_{in\text{-}vitro}$]) was collected at 3 m depth and every 2-3 weeks from mid-February to mid-June few meters away from where the C3 sensor was attached. For nitrate analyses, triplicate water samples were filtered with a 0.8 µm polycarbonate filter, where the filtrate water was immediately kept in a centrifuge tube and stored frozen at -20ºC. Nitrate analyses were determined in the laboratory using a continuous flow automated analyzer (CFA, Auto-Analyzer 3, SEAL). For [$Chla_{in\text{-}vitro}$], seawater was filtered (0.25-0.5 L) onto a Whatman GF/F glass fiber filters, and immediately double-folded, wrapped in aluminum foil and stored at -20ºC for *a posteriori* analyses in the laboratory. For a fluorometric determination of [$Chla_{in\text{-}vitro}$], frozen filters were placed in glass vials with 100% methanol for few hours on a dark fridge at 10°C. For [$Chla_{in\text{-}vitro}$], the extracted solvent was determined using the Turner Designs Trilogy fluorometer (model: 7200-000) and the non-acidification method (Fragoso et al., 2019). For phytoplankton identification and quantification, water samples were fixed with neutral Lugol's iodine solution to a final concentration of ~1% into dark amber bottles and stored at room temperature and in the dark for later microscopic analyses in the laboratory.

197 ## 2.3 USV AutoNaut sampling

198

199 The AutoNaut is a commercially available USV that relies on sea surface waves to
200 produce forward thrust, making it suitable for sustained operations at sea without human
201 assistance. Along with the instrumentation needed for navigating autonomously, the vehicle
202 carries several scientific payload integrated on the USVs hull and keel (between 25 and 50 cm
203 approximately below the waterline) that collects information about a wide range of
204 environmental variables. Among these, we had an Eco Triplet sensor (Wet Labs, Oregon, USA)
205 to measure *FChla* (λ_{ex}= 470 nm, λ_{em}= 695 nm), turbidity (λ= 700 nm) and fluorescence of
206 colored dissolved organic matter (*CDOM*, λ_{ex}= 370 nm, λ_{em}= 460 nm). A manufacturer
207 calibration factor converted the units of *FChla* to [*Chla*] (mg m^{-3}), *CDOM* to ppb and turbidity to
208 Nephelometric Turbidity Units (NTU). In addition, the USV was equipped with a Seabird CTD
209 SBE 49 (sampling rate of 16 Hz) for measurements of temperature and salinity and an oxygen
210 Optode 4835 (Aanderaa) for oxygen concentration (µM, later converted to mg L^{-1}). Finally, a
211 weather station (Airmar 220WX) for measurements of wind speed was located on the mast of the
212 USV. The USV was deployed from the Mausund field station (located north of Frøya island, in
213 the south-western part of Frohavet, Fig. 1) on 12th April 2022 and navigated in Frohavet until
214 28th April 2022. The log files of each sensor were converted to CSV format and merged in
215 Python. Data was binned for every minute.

216 ## 2.4 Non-photochemical quenching correction

217

218 *In vivo* (in situ) *FChla* is commonly used as a proxy for phytoplankton biomass.
219 However, when phytoplankton cells are usually exposed to high irradiance (particularly around

noon), excess energy is dissipated as heat, reducing the *FChla* signal in the water (Travers-Smith et al 2021). This photophysiological process is called non-photochemical quenching (*NPQ*) (reviewed by Brunet et al., 2011)). To visualize the overall trend of corrected *FChla*, the beginning of each *NPQ*-induced trough was connected linearly to the end of the trough, resulting in a straight line over the period affect by *NPQ*. This method excludes the *FChla* suppressed by *NPQ* and ignores small variability of *FChla* during the day, however, it suits well to show general trends of bloom dynamics (before, peak and post-bloom) in April 2022.

2.5 Satellite observations

Sentinel-3 images from OLCI (Ocean and Land Colour Instrument) sensor (multispectral imager) are used to provide an overview of the sampling region, and to assess whether the USV is observing spatial or temporal variations in the *FChla*. To determine the daily pattern of *Chla*, all the Sentinel-3 *Chla* maps which contain the target region during the day were downloaded and merged. The images are resampled to the same spatial grid and averaged. Pixels which displayed land or clouds were excluded from the averaging process.

2.6 Mixed Layer Depth

Mixed layer depth was calculated from data from SINMOD, a 3D ocean model system. The model has been established for the coastal region outside mid-Norway with a high spatial resolution (800m). SINMOD's hydrodynamic component utilizes the primitive Navier-Stokes equations to calculate ocean properties such as water current, velocity, water temperature, and

pressure (see Slagstad & McClimans, 2005 for more details on the hydrodynamic module). The model is established on a z/z*-grid with fixed horizontal grid size and nesting for high spatial resolution. The North Atlantic and Arctic region are modeled with a 20 km resolution, which produces boundary conditions for a higher resolution configuration of 4 km horizontal grid size for the Nordic Seas and further to 800 m grid size for the coastal region outside Mid-Norway. The 20 km model uses specified boundary conditions, including 12 tidal components at open boundaries, with data imported from the TPXO tidal model for global ocean tides. Interpolated ERA5 atmospheric data from ECMWF (for more details see Hersbach et al. (2020) is used to force the ocean model domain, including 3 hourly wind forcing, air pressure, and daily air temperature, humidity, and cloud cover to calculate heat exchange. Norwegian freshwater discharges from rivers and land are applied using data from simulations by the Norwegian Water Resources and Energy Directorate with a version of the HBV-model (Beldring et al., 2003), while historic data from SMHI Hype model data is used for other European rivers (https://hypeweb.smhi.se/). For more information, refer to Hersbach et al. (2020). Mixed layer depth is calculated from the SINMOD output as the depth at which the density gradient exceeds 0.01 kg m^{-1}.

3 Results

3.1 Mooring buoy data

Integrated daily irradiance above water from HOBO light loggers (converted from klux to µmol photons m^{-2} s^{-1}, see methods) gradually increased from mid-February to mid-June, showing peak in values (up to 2×10^4 µmol photons m^{-2} s^{-1}) from early April until early May (Fig. 2a).

This suggests a period of consistent clear and sunny skies in April for at least 2 weeks. Average wind speed varied in the region of Frohavet from February until mid-June (Fig. 2b). Average wind speed was particularly strong (up to 20 m s^{-1}) during March and early April (Fig. 2b). From mid-April until late April (time when the USV AutoNaut was in Frohavet, Fig. 2e), average wind speed was relatively weak for several days (< 5 m s^{-1}) compared to March. Concomitantly, seawater temperature from a buoy (~3 m deep) located near the coast of Frøya island (Fig. 1) gradually increased from early April until late June and shortly increased from ~ 6 to 8°C in mid-April (Fig 2c). Chlorophyll a concentrations ($FChla_{BUOY}$) and turbidity from the buoy station near Frøya island (Fig. 1) gradually increased from mid-March and peaked from mid to late April. The spring bloom (March-June) consisted of multiple peaks (Fig. 2d) - a short peak in late March where the haptophyte *Phaeocystis* sp. dominate the bloom and a second long peak during April where diatom *Skeletonema* spp. is the dominant genus (Table S1. Supplementary material). The USV AutoNaut was located in Frohavet before, during and after the *Skeletonema* bloom in April (Fig. 2e), capturing the temporal and spatial dynamics of the bloom.

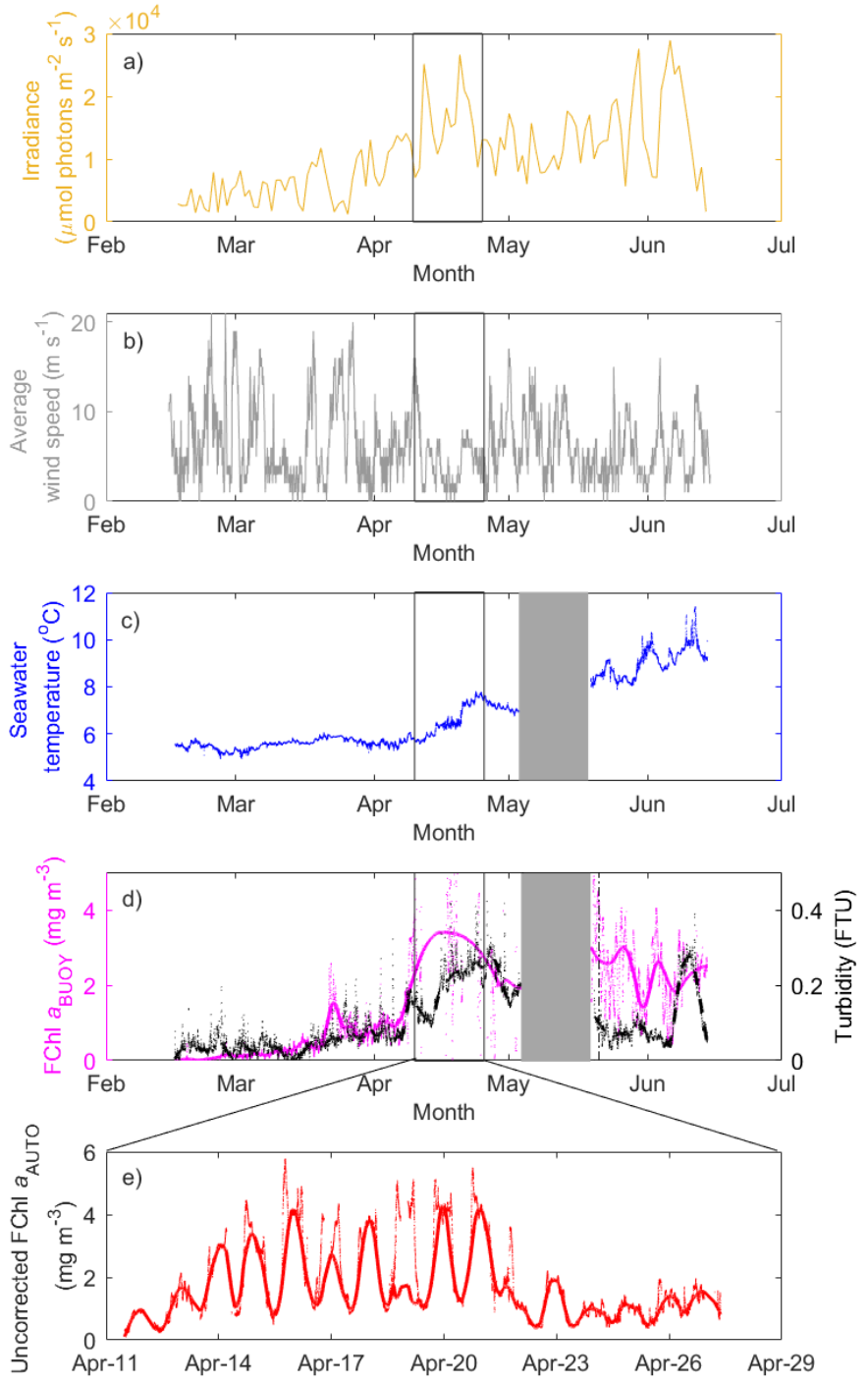

Figure 2- Time series of environmental parameters and the spring phytoplankton bloom. a) integrated daily irradiance (µmol photons m^{-2} s^{-1}), b) average wind speed (m s^{-1}), c) temperature (°C), d) *in vivo* chlorophyll (mg m^{-3}) and turbidity (FTU) from the stationary buoy from mid-February until mid-June 2022 and e) uncorrected *in vivo* chlorophyll from the AutoNaut from April 11th – April 28th. Grey box in b) and c) represents lack of data due to malfunctioning of the instrument. For d) and e) dot represent the median-calculated data from seven consecutive runs and line represents the smoothing parameter (*rloess* method in Matlab).

289

290 ### 3.2 Daily variation of $FChla_{AUTO}$

291

292 $FChla_{AUTO}$ (mg m^{-3}) varied with time, with low values around 12th April (<1 mg m^{-3}), increasing
293 gradually until 16th April, reaching maximum average values ~ 4 - 5 mg m^{-3} and decreasing
294 again on the 23rd – 24th April (average ~ 1 mg m^{-3}) (Fig. 2d). $FChla_{AUTO}$ (mg m^{-3}) varied also as a
295 function of irradiance during the day cycle, showing low values when irradiance is the highest
296 (around noon) (Fig. 3a). Such low $FChla_{AUTO}$ daylight values occurred due to *NPQ*. To correct
297 for this values, linear interpolation of night $FChla_{AUTO}$ was used, to show the robust trends in
298 [*Chla*] chlorophyll concentration before, during and after the bloom (Fig. 3b).

299

300

301

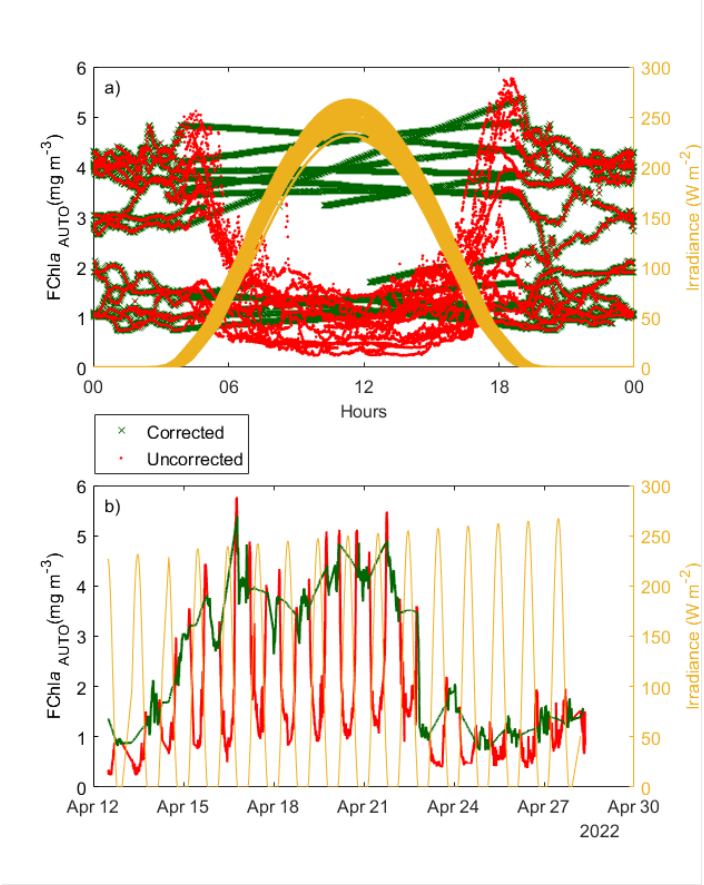

Figure 3- Daily and temporal variations of *in situ* chlorophyll *a* fluorescence (*FChla*$_{AUTO}$ (mg m^{-3})) and modelled irradiance. a) Time series and b) daily cycle of *FChla*$_{AUTO}$ uncorrected (red) and corrected for non-photochemical quenching (green) from the USV AutoNaut and modelled daily irradiance (yellow) derived from 12th – 28th April 2022.

3.3 USV AutoNaut

The USV AutoNaut was present in surface waters of Frohavet from April 11th – April 27th (Fig. 4a). The USV departed from a small island, Mausund, north of Frøya island and moved towards the deep waters of Frohavet. The USV initially moved out of Mausund Island and northwards around 15th April, along Froan archipelago, then east around 19th April, then south (east of Frøya) on April 23rd, completing its mission around the center, deep waters of Frohavet (Fig. 4a). Corrected $FChla_{AUTO}$ (mg m^{-3}) gradually increased from April 11th, reaching its peak (up to 5.5 mg m^{-3}) on ~ April 16th until ~ April 22nd when it abruptly declined, and reaching low values (< 2 mg m^{-3}) (Fig. 4b). Average turbidity values were lower than 0.2 (NTU) from April 11th – April 12th, slightly increasing during the period of the bloom (average > 0.2 NTU). Turbidity values were less 'noisy' from 14th - 20th April and gradually declined until 23rd April, becoming again noisier and around 0.2 NTU afterwards. Sea surface temperature (SST), colored dissolved organic matter (CDOM) and dissolved oxygen (DO) gradually increases from April 11th until April 18th (~ 6 - 9°C for SST, 1.1-2.2 ppb for CDOM and 9.7 - 13 mg L^{-1} for DO). Concomitantly, salinity and average wind speed (m s^{-1}) decrease from 34 to 32 and from 10 m s^{-1} until 3 ms^{-1}, respectively. Salinity sharply increases from 32 to 33 and CDOM and SST abruptly decreases on April 19th, from 2.1 to 1.2 ppb and 8.9-7.5, respectively. At the same period (particularly on April 20th, wind speed peaks up, reaching > 10 m s^{-1}). From April 18th onwards (until April 26th), SST, CDOM, salinity and wind speed fluctuate. DO reach highest values on April 19th and 20th and sharply goes down to < 10 mgL^{-1} after April 23rd.

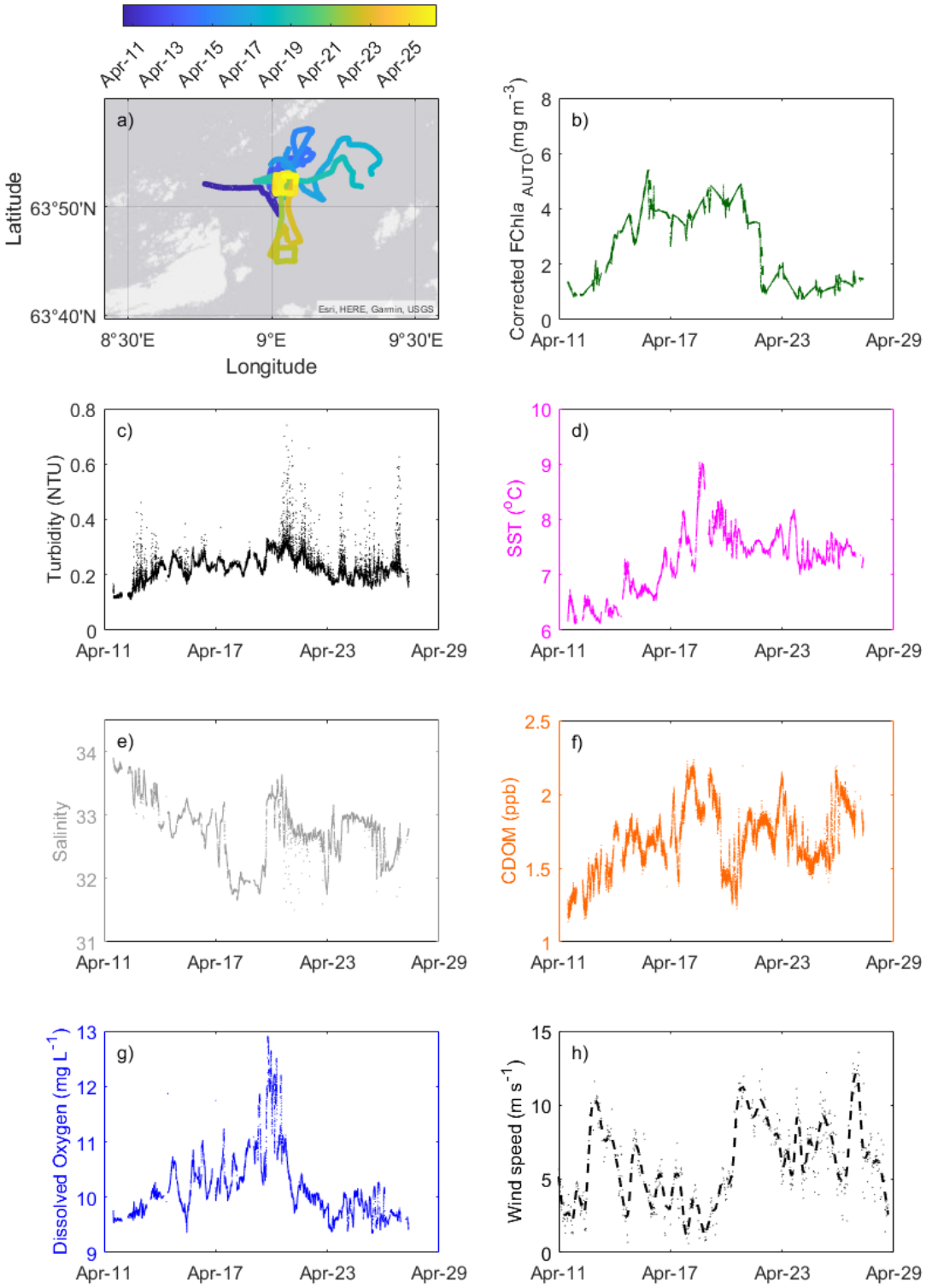

Figure 4- Track of the USV AutoNaut and the environmental parameters collected. a) Frohavet region and the track line of the USV AutoNaut from 11th – 28th April. Time series of b) corrected chlorophyll a fluorescence ($FChla_{AUTO}$ (mg m^{-3})), c) turbidity (NTU), d) sea surface temperature (SST (°C)), e) salinity, f) colored dissolved organic matter (CDOM (ppb)), g) dissolved oxygen (mg L^{-1}), and h) wind speed (m s^{-1}) from the USV AutoNaut.

3.4 Satellite images and USV AutoNaut track

To verify whether the bloom variability detected by the USV AutoNaut is temporal (e.g. start, peak and collapse) or spatial (patchiness), daily satellite images along with the USV tracks were analyzed together (Fig. 5). According to satellite images and, in alignment with the observations from the USV, the bloom started from ~ April 7th – 18th, peaked ~ April 21st, declined on April 24th, where the USV was confined in relatively low [*Chla*] regions (< 1 mg m^{-3}) and collapsed on April 26th (Fig. 5).

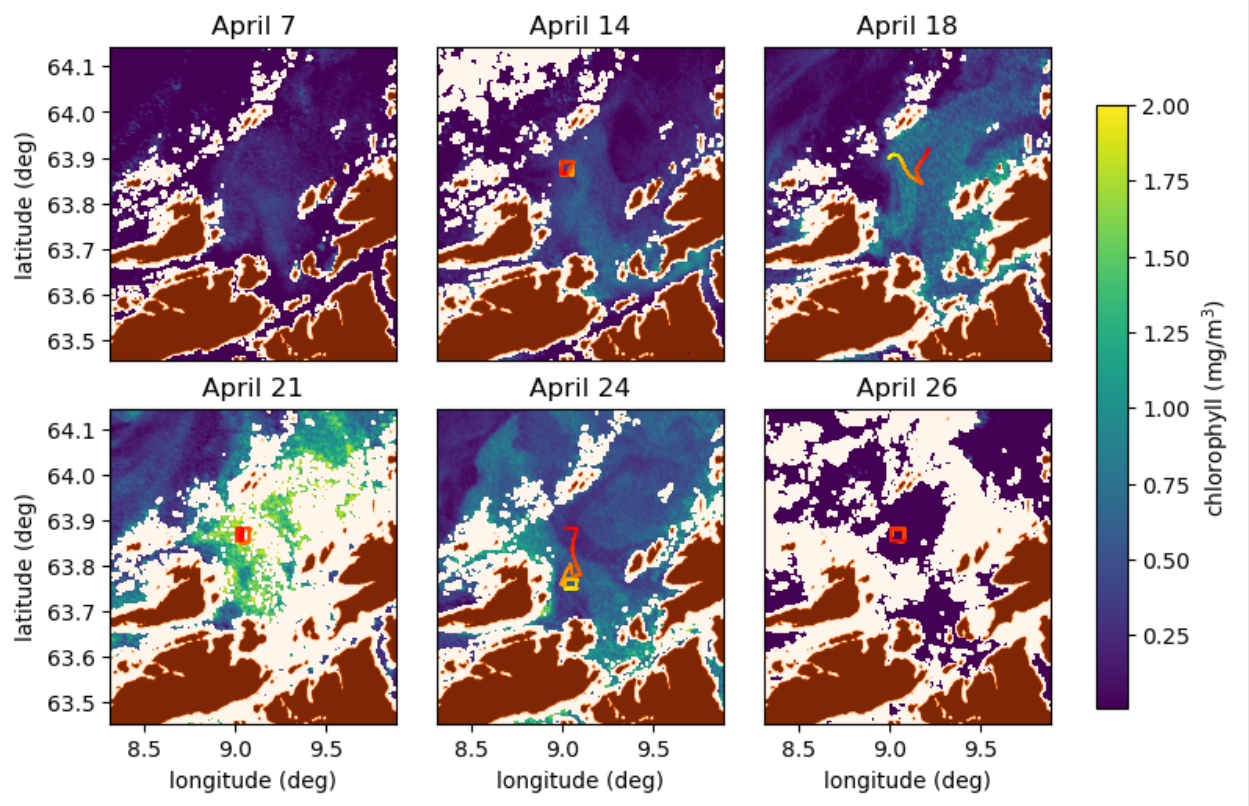

Figure 5 - Satellite images (Sentinel 3) of chlorophyll *a* concentrations (mg m^{-3}). Spatial and temporal variability of [*Chla*] in Frohavet region on April 7th, 14th, 18th, 21st, 24th and 26th. Note the tracking path of the USV AutoNaut for each day, during early (yellow) to late (red) hours.

3.5 Correlation of USV AutoNaut parameters

The phytoplankton bloom observed as corrected $FChla_{AUTO}$ seemed, in general, not to be concentrated within a certain water mass, being widely present in waters with low and high salinity and temperature values (Fig. 6a and 6c). The phytoplankton bloom seemed to, rather, have a temporal trend, starting from 12-13th April and ending on 21st April. Salinity and CDOM presented a negative relationship, changing progressively in values in the early phase of the bloom (Fig. 6a and 6b). Temporally, the USV AutoNaut traveled waters with a wide range of salinity and temperature in the beginning of the mission, concentrating later in the center of Frohavet (after April 19th – salinities are between 32 and 33) (Fig. 6d). Lowest daily turbidity values had a positive relationship with DO and chlorophyll (Fig 6e and 6f). Waters with high dissolved oxygen levels (> 11 mg L^{-1}) had less variability (which coincided with a period of weak winds and high chlorophyll concentrations) (Fig. 4c and 4h).

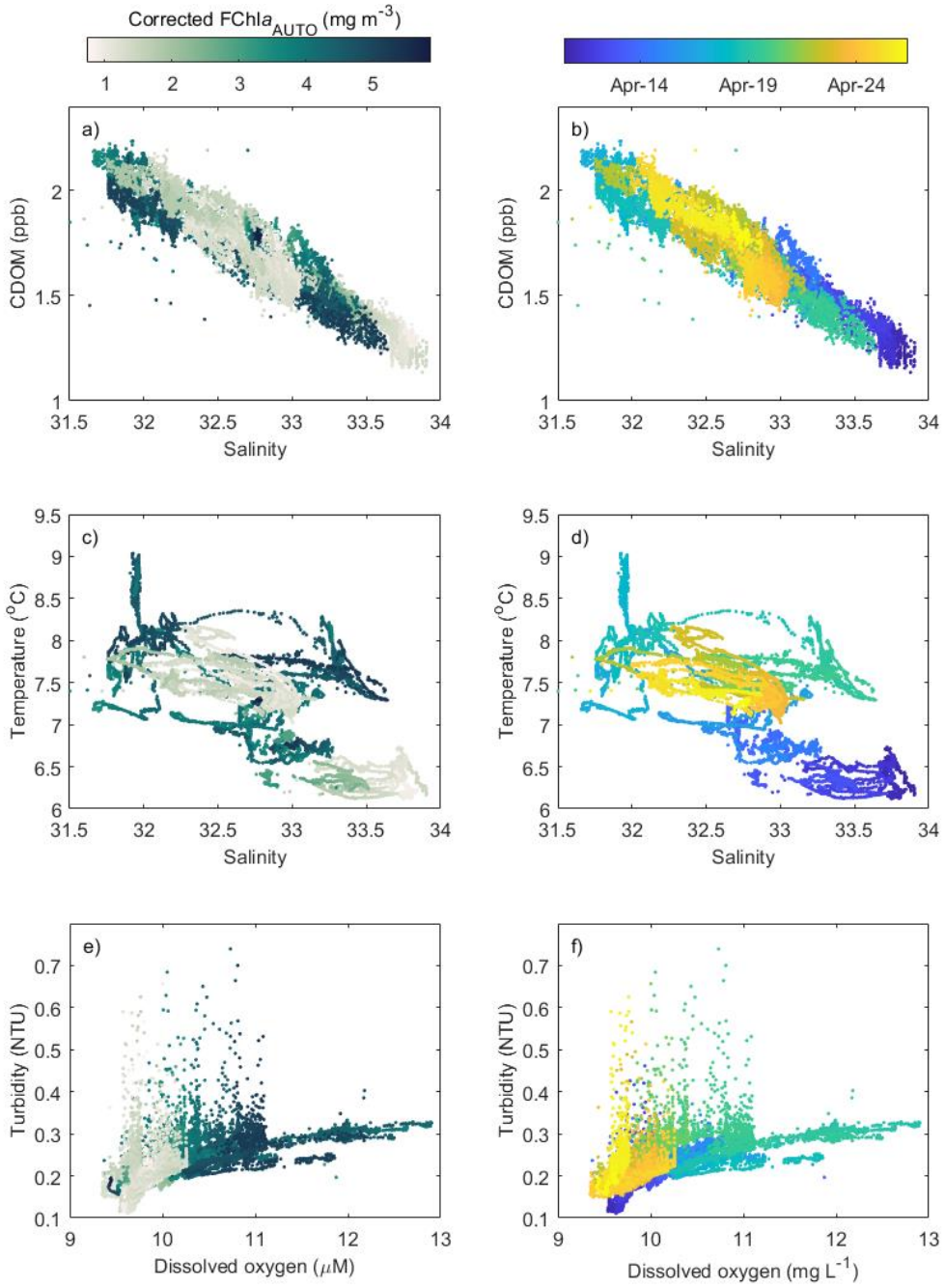

365

366 **Figure 6- Correlation plots between parameters from the USV AutoNaut.** Correlations
367 between a,b) salinity and coloured dissolved organic matter (CDOM (ppb)), c,d) salinity and
368 temperature (°C) and e,f) dissolved oxygen (mg L^{-1}) and turbidity (NTU) as function of
369 *FChla$_{AUTO}$* (left) and time (right) from the USV AutoNaut.
370

371

372 Values of corrected $FChla_{AUTO}$ varied as a function of wind during the period that the
373 USV AutoNaut was in Frohavet (Fig. 7). During a pre-bloom condition (~April 11^{th} – 13^{th}),
374 average wind speed was variable (from 1-10 m s^{-1}), followed by a blooming period (> 2 mg m^{-3}),
375 where corrected $\underline{FChla}_{AUTO}$ values from the USV AutoNaut rapidly increase in a few days
376 (~April 13^{th} – 15^{th}). During the blooming period average wind speed was low (< 6 m s^{-1}), while
377 DO and turbidity were high (> 10 mg L^{-1} for DO and > 0.2 NTU for turbidity) (Fig 7c,d). After
378 this period, here referred as 'transitional period', winds started to pick up (average speed from 7
379 to 13 m s^{-1}), while chlorophyll concentration and turbidity were still high (> 4 mg m^{-3} for
380 corrected $FChla_{AUTO}$ and 0.25 NTU for turbidity) (Fig. 7). The transitional period was followed
381 by a post-bloom period, where chlorophyll values were low (< 2 mg m^{-3}) but average winds were
382 still high (from 5 – 13 m s^{-1}) (Fig. 7b).

383

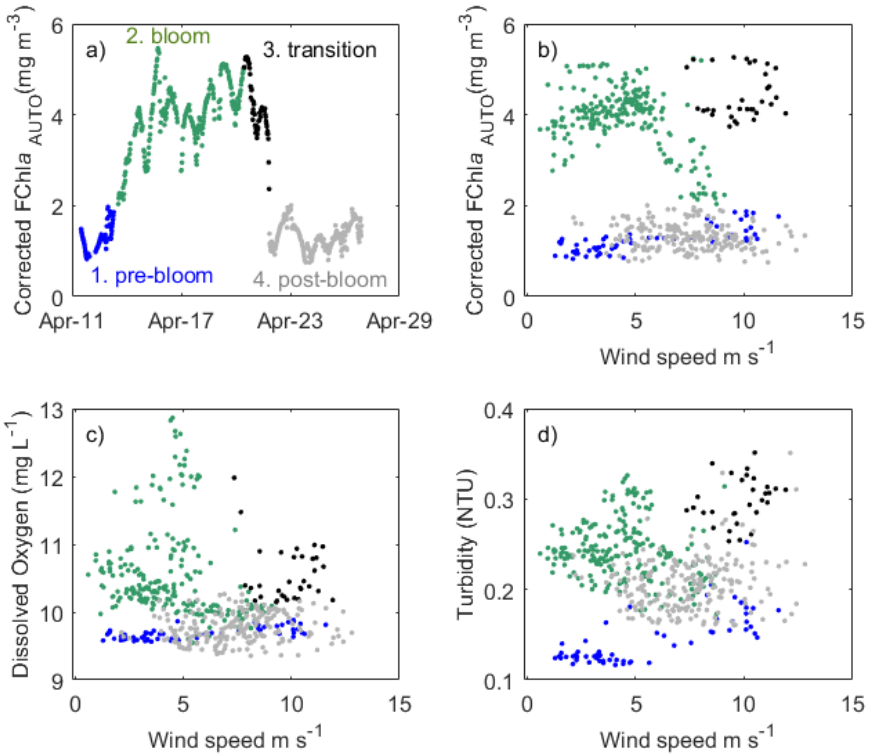

Figure 7- Correlation plots of parameters from the USV AutoNaut. Correlation plots between a) year day and corrected chlorophyll fluorescence ($FChla_{AUTO}$ (mg m^{-3})), b) wind speed (m s^{-1}) and corrected chlorophyll fluorescence ($FChla_{AUTO}$ (mg m^{-3})), c) wind speed (m s^{-1}) and dissolved oxygen (mg L^{-1}) and d) wind speed (m s^{-1}) and turbidity (NTU).

390

391 ### 3.6 Discrete water sampling and modelled mixed layer depth

392

393 Nitrate concentrations from discrete water samples collected at the coast of Frøya, where the
394 buoy is located (Fig. 1), showed an overall continue decline from mid-February until mid-June
395 with pulses of nutrient occurring on April 5th and May 4th (6 and 4 µM, respectively, Fig. 8a).
396 Values of [$Chla_{in\text{-}vitro}$] increased with time, with a decline on May 4th (< 2 µg L^{-1}, Fig. 8b), which
397 coincided with the post bloom period observed after the USV AutoNaut was in the water.
398 Modelled mixed layer depth was shallow (< 15 m), particularly during the period of bloom
399 development, when the USV AutoNaut was in the water (Fig. 8c).

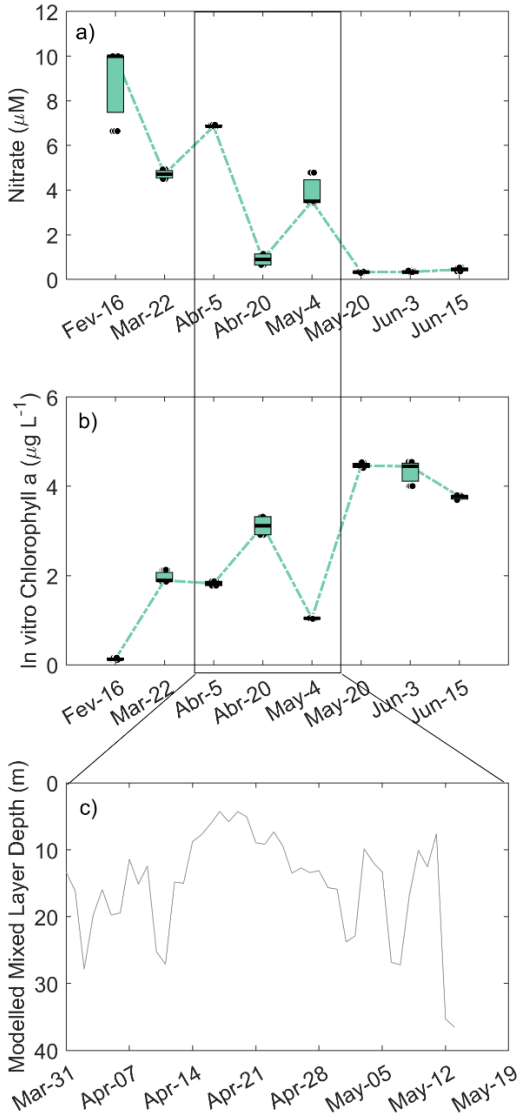

Figure 8- Nitrate, in vitro chlorophyll *a* concentrations and mixed layer depth as a function of time. Time series of a) nitrate concentrations (µM) and b) *in-vitro* chlorophyll *a* from discrete water samples collected at 3 m depth from near Frøya island (µg L^{-1}). c) Modelled average mixed layer depth (MLD) from 31st March – May 13th derived from SINMOD simulations. Location of Frøya and regions of modelled MLD simulation is shown in Figure 1 (circle symbol).

4 Discussion

4.1 Non-photochemical quenching

In vivo *FChla* signal varied widely in this study as a function of daily irradiance. Non-photochemical quenching clearly affected the $FChla_{AUTO}$ signal during daytime, appearing low when irradiance is high (peak at noon), while being stable during nighttime. Methods for *NPQ* correction from fluorometers installed on mobile (e.g. gliders and BCG-Argo floats) and moored platforms (e.g. vertical profilers and buoys) have been established (Fragoso et al., 2021; Lucius et al., 2020; Xing et al., 2018). Each of these methods follows their own set of assumption, given that not all set of parameters are measured from distinct platforms. For semi-autonomous observations (e.g. USVs), interpolation of unaffected nighttime *FChla* signal has been applied in this and other studies to correct for *NPQ* (Scott et al. (2020). In Scott et al. (2020), daytime *FChla* from the USV Saildrone was corrected using the proportion of *FChla* to Volume Scattering Function (β, 124°, 650 nm) from the night before and after the *NPQ* event and assumed that daytime β measurements are not influenced by *NPQ*. As suggested by the authors, this method is only appropriate under a close examination of the types of water masses. That is because it assumes a consistent temporal and spatial distribution of factors that influences β, such as detritus, sediments and phytoplankton. In our study, this method was not suitable due the noisy turbidity measurements (particularly when wind speed was high), suggesting the influence of air bubbles and particles, such as sediments and detritus in the backscattering signal. Although phytoplankton constitutes a significant portion of particles in productive waters of the coast of mid-Norway, other particles, including zooplankton, fecal pellets, sediments and detritus can be

highly heterogeneous in space and time, influencing the backscattering signal (Fragoso et al., 2019; Fragoso et al., 2021). Thus, for $FChla_{AUTO}$ corrections in this study, daily measurements were based the percent reduction in $FChla_{AUTO}$ by modelled irradiance. This method is only appropriate to observe daily trends in $FChla_{AUTO}$, rather than sub-mesoscale patchiness of phytoplankton distributions occurring less than a day.

4.2 Phytoplankton bloom dynamics

The spring bloom (March-June) in Frohavet consisted of multiple peaks - a short one in late March dominated by the haptophyte *Phaeocystis*, a second long one (2 weeks) during April (where diatom *Skeletonema* spp. is the dominant) and a third 'on-and-off' bloom until late June dominated again by *Skeletonema*. Multiple biomass peaks composed of the same taxa (in this case *Skeletonema*) or assemblages of taxa are likely a response of the dynamic nature of this region. In these places, distinct stochastic drivers (nutrient pulse, a period of calm weather, heatwaves, grazing selection etc.) determine the timing of peaks over a short period of time (Type 4 blooms as described in Isles and Pomati, 2021). This means that for each of these blooms observed in during spring to summer in Frohavet, distinct abiotic (changes in nutrient and light conditions) and biotic factors (grazing pressure) might have shaped the intensity, composition and duration of those blooms.

The USV was in the water in April during the second long $FChla_{BUOY}$ peak (2 weeks) and captured the temporal and spatial dynamics of *Skeletonema* bloom before, during and after its recession. During this period, a rise in $FChla_{AUTO}$ from the USV AutoNaut occurred concomitantly with a rise in SST and [CDOM] as well as with a decrease in salinity values and

wind speed, suggesting that sunny skies, calm winds and warmer temperatures promoted snow melt and high freshwater input from river run off along the coast. Thus, light was the environmental driver that likely promoted this bloom, since several days of clear skies and relatively calm winds shoaled the mixing layer after intense wind mixing and prolonged period of low light conditions of Norwegian winter. In the North Atlantic, similar conditions were observed where a dramatic increase in cellular division rates (net population growth rate from 0.02 to 0.08 divisions d^{-1}) over a short period of time (9 days) occurs as a consequence of the rapid shoaling of the mixed layer during calm weather periods, consistent with Sverdrup's paradigm (Mignot et al., 2018). In Frohavet, $FChla_{BUOY}$ started to accumulate since mid-March, but it was not until mid-April that a proper bloom was observed, where concentrations changed from 1 to 5 mg m^{-3} in 5 days.

While the spring bloom in this study developed exponentially with 5 days, the collapse of the bloom was rather quick, 1-2 days. *Skeletonema* sp. is an ubiquitous fast-growing diatom (Lundsør et al., 2022), and it is possible that nutrient limitation after intense growth could have caused of the collapse of the bloom. However, due to the intermittent changes and dynamic nature of weather conditions of the coast of mid-Norway, particularly from winter to spring transition, it is likely that strong wind speed and deepening of the mixing layer (after 2 weeks of calm weather) paused the bloom development. This could initially dilute the accumulated biomass and consequently reduced the availability of light for the phytoplankton growth. Similar conditions were observed in the Northwestern Mediterranean Sea, where subsequent storms and vertical mixing due to the intermittent changing weather conditions from winter to spring cause the collapse of spring blooms (Keerthi et al., 2021). In this study, the evidence of a storm surge shown by the sudden increase in average wind speed and increased nutrient availability at the

surface in early May indicates that vertical mixing likely promoted the rapid decline of the bloom.

Zooplankton abundance and top-down pressure is evident in the coast of mid-Norway, particularly during summer (Fragoso et al., 2022). Although light might have induced phytoplankton cellular division to optimum levels, slight lags (few days) in zooplankton grazing might have been another reason why phytoplankton accumulation reached a peak (3-4 days), where grazing rates outbalanced phytoplankton division and growth. This suggests that loss processes, such as grazing, can also be rather fast, highlighting the need of highly temporal and spatial-resolved measurements in dynamic regions. The copepod *Calanus finmarchicus* is the dominant mesozooplankton species in the Norwegian Sea and abundance has strongly been correlated with chlorophyll *a* concentration, suggesting tight coupling in other regions of the coast of Norway (Dong et al., 2022). Microzooplankton, such as ciliates and heterotrophic dinoflagellates, have a short generational time and high rates of predation, where slight lags in the response of these predators might have allowed for the positive accumulation rates during the initial state of the bloom (Mojica et al., 2021). Thus, it is likely that grazing might have slowed down further accumulation of phytoplankton biomass ([Chl a]) and bloom development, particularly in shallow mixed layers, which favors predator-prey encounter rates. Although the short-scale (few days) mismatch between phytoplankton and zooplankton abundances might have some influence in the development and collapse of the bloom, it is still likely that increase in average wind speed was the main obvious cause, given the fast (1-2 days) decline in chlorophyll concentrations from 5 to 1 mg m^{-3}.

4.3 Submesoscale patchiness

High frequency-resolved mobile platforms such as the USV AutoNaut is a great tool to examine the sub-mesoscale variability of water masses, revealing the patchiness of the system (Dallolio et al., 2021). The wide range in salinity (31.5 - 34°C), temperature (6 - 9°C) and CDOM (1 - 2.5 ppb) reveals that the USV AutoNaut travelled through many distinct water masses, some with more or less influence of riverine input from Trondheimsfjord. Satellite images revealed that phytoplankton spatial distribution in Frohavet is highly patchy over the bloom period, but temporal changes, such as the start ~ April 7th, peak on April 21st, suppress on April 24th and collapse on April 26th were more prominent. The phytoplankton bloom was patchy, particularly on April 24th but did not appear to be confined to a certain water mass, rather transitioning in time and associated to wind conditions (low wind speed - accumulation and high wind speed – disruption of the bloom). This suggests that in spite of some degree of spatial variability observed in environmental factors (salinity and temperature, for example), the formation and decline of the bloom (from <1 to 6 mg m^{-3}) was rather temporal due the fast changes in the environment (increase of wind strength).

5 Conclusions

Here we showed the detailed dynamics of a phytoplankton spring bloom in a complex productive region of the coast of Norway using an integrative observational approach. We observed a rapid

(5 days) bloom development (from 1 to 5 mg m^{-3}) dominated by the diatom *Skeletonema* occurring in spells of 'good weather', meaning few days of sunny, clear skies and weak winds in the middle of 'stormy spring', typical of high latitudinal regions. The collapse of this bloom was even faster, occurring in 1-2 days, concomitant with increase in wind speed, suggesting the strong influence of environmental conditions in the spring bloom.

Integrative approaches using of multiple ocean observation platforms (referred as the observational pyramid in Williamson et al., 2023) is essential to capture the short-term changes of phytoplankton in space and time. As climate continues to change, fluctuations in the environmental conditions (e.g. storm, floods, heatwaves) will likely become more and more frequent, and thus, the response of plankton communities, will likely become more extreme. Therefore, the combination of sensor-based technology and traditional methods for validation and monitoring of the ocean is fundamental to understand of the interlink and tipping points of phytoplankton dynamics to multiple environmental stressors related to climate change.

Acknowledgments

We thank Seaweed Solution for providing the irradiance data, assistance and resources for collection of water samples in the coast of Frøya. Many thanks to the staff of Mausund Feltstasjon for providing the infrastructure for deployment and recovery of the USV AutoNaut. Contributions by all authors are from the Center of Excellence for Autonomous Marine Operation and Systems (AMOS) at NTNU (NRC, Project 223254). This work was supported by the Research Council of Norway through the Centre of Excellence funding scheme (NTNU

AMOS, grant no. 223254), AWAS (327670) and MoniTARE (315514). The authors have no financial conflicts of interests.

Open Research

Our observational data of the parameters measured with the AutoNaut in Frohavet are available at 10.5281/zenodo.8283108.

References

Alkire, M. B., Lee, C., D'Asaro, E., Perry, M. J., Briggs, N., Cetinić, I., & Gray, A. (2014). Net community production and export from Seaglider measurements in the North Atlantic after the spring bloom. *Journal of Geophysical Research: Oceans, 119*(9), 6121–6139. https://doi.org/10.1002/2014JC010105

Behrenfeld, M. J. (2010). Abandoning Sverdrup's Critical Depth Hypothesis on phytoplankton blooms. *Ecology*, *91*(4), 977–989. https://doi.org/10.1890/09-1207.1

Behrenfeld, M. J., & Boss, E. S. (2014). Resurrecting the ecological underpinnings of ocean plankton blooms. *Annual Review of Marine Science*, *6*, 167–194. https://doi.org/10.1146/annurev-marine-052913-021325

Behrenfeld, M. J., Doney, S. C., Lima, I., Boss, E. S., & Siegel, D. A. (2013). Annual cycles of ecological disturbance and recovery underlying the subarctic Atlantic spring plankton bloom. *Global Biogeochemical Cycles, 27*(2), 526–540. https://doi.org/10.1002/gbc.20050

Behrenfeld, M. J., Hu, Y., O'Malley, R. T., Boss, E. S., Hostetler, C. A., Siegel, D. A., et al.

(2017). Annual boom–bust cycles of polar phytoplankton biomass revealed by space-based lidar. *Nature Geoscience*, *10*(2), 118–122. https://doi.org/10.1038/ngeo2861

Beldring, S., Engeland, K., Roald, L. A., Sælthun, N. R., & Voksø, A. (2003). Estimation of parameters in a distributed precipitation-runoff model for Norway. *Hydrology and Earth System Sciences*, *7*(3), 304–316. https://doi.org/10.5194/hess-7-304-2003

Boss, E., & Behrenfeld, M. (2010). In situ evaluation of the initiation of the North Atlantic phytoplankton bloom. *Geophysical Research Letters*, *37*(18), n/a-n/a. https://doi.org/10.1029/2010GL044174

Brunet, C., Johnsen, G., Lavaud, J., & Roy, S. (2011). Pigments and photoacclimation processes. In C. A. Llewellyn, E. S. Egeland, G. Johnsen, & S. Roy (Eds.), *Phytoplankton Pigments: Characterization, Chemotaxonomy and Applications in Oceanography.* (pp. 445–71). Cambridge: Cambridge University Press.

Carberry, L., Roesler, C., & Drapeau, S. (2019). Correcting in situ chlorophyll fluorescence time-series observations for nonphotochemical quenching and tidal variability reveals nonconservative phytoplankton variability in coastal waters. *Limnology and Oceanography: Methods*, *17*(8), 462–473. https://doi.org/10.1002/lom3.10325

Chiswell, S. M., Calil, P. H. R., & Boyd, P. W. (2014). Spring blooms and annual cycles of phytoplankton: A unified perspective. *Journal of Plankton Research*, *37*(3), 500–508. https://doi.org/10.1093/plankt/fbv021

Dallolio, A., Quintana-Diaz, G., Honoré-Livermore, E., Garrett, J. L., Birkeland, R., & Johansen, T. A. (2021). A Satellite-USV System for Persistent Observation of Mesoscale Oceanographic Phenomena. *Remote Sensing*, *13*(16), 3229. https://doi.org/10.3390/rs13163229

Dong, H., Zhou, M., Raj, R. P., Smith, W. O., Basedow, S. L., Ji, R., et al. (2022). Surface chlorophyll anomalies induced by mesoscale eddy-wind interactions in the northern Norwegian Sea. *Frontiers in Marine Science*, *9*(September), 1–14. https://doi.org/10.3389/fmars.2022.1002632

Edwards, M., & Richardson, A. J. (2004). Impact of climate change on marine pelagic phenology and trophic mismatch. *Nature*, *430*(7002), 881–884. https://doi.org/10.1038/nature02808

Fragoso, G M., Davies, E. J., Fossum, T. O., Ullgren, J. E., Majaneva, S., Aberle, N., et al. (2022). Contrasting phytoplankton-zooplankton distributions observed through autonomous platforms, in-situ optical sensors and discrete sampling. *PLOS ONE*, *17*(9), e0273874. https://doi.org/10.1371/journal.pone.0273874

Fragoso, Glaucia M., Davies, E. J., Ellingsen, I., Chauton, M. S., Fossum, T., Ludvigsen, M., et al. (2019). Physical controls on phytoplankton size structure, photophysiology and suspended particles in a Norwegian biological hotspot. *Progress in Oceanography*, *175*, 284–299. https://doi.org/10.1016/j.pocean.2019.05.001

Fragoso, Glaucia M., Johnsen, G., Chauton, M. S., Cottier, F., & Ellingsen, I. (2021). Phytoplankton community succession and dynamics using optical approaches. *Continental Shelf Research*, *213*(November 2020), 104322. https://doi.org/10.1016/j.csr.2020.104322

González-Gil, R., Banas, N. S., Bresnan, E., & Heath, M. R. (2022). The onset of the spring phytoplankton bloom in the coastal North Sea supports the Disturbance Recovery Hypothesis. *Biogeosciences*, *19*(9), 2417–2426. https://doi.org/10.5194/bg-19-2417-2022

Henson, S. A., Cole, H. S., Hopkins, J., Martin, A. P., & Yool, A. (2018). Detection of climate change-driven trends in phytoplankton phenology. *Global Change Biology*, *24*(1), e101–

e111. https://doi.org/10.1111/gcb.13886

Hersbach, H., Bell, B., Berrisford, P., Hirahara, S., Horányi, A., Muñoz-Sabater, J., et al. (2020). The ERA5 global reanalysis. *Quarterly Journal of the Royal Meteorological Society*, *146*(730), 1999–2049. https://doi.org/10.1002/qj.3803

Huot, Y., & Babin, M. (2010). Overview of Fluorescence Protocols: Theory, Basic Concepts, and Practice. In *Chlorophyll a Fluorescence in Aquatic Sciences: Methods and Applications* (pp. 31–74). Dordrecht: Springer Netherlands. https://doi.org/10.1007/978-90-481-9268-7_3

Isles, P. D. F., & Pomati, F. (2021). An operational framework for defining and forecasting phytoplankton blooms. *Frontiers in Ecology and the Environment*, *19*(8), 443–450. https://doi.org/10.1002/fee.2376

Johnsen, G., Norli, M., Moline, M., Robbins, I., von Quillfeldt, C., Sørensen, K., et al. (2018). The advective origin of an under-ice spring bloom in the Arctic Ocean using multiple observational platforms. *Polar Biology*, (0123456789). https://doi.org/10.1007/s00300-018-2278-5

Keerthi, M. G., Lévy, M., & Aumont, O. (2021). Intermittency in phytoplankton bloom triggered by modulations in vertical stability. *Scientific Reports*, *11*(1), 1285. https://doi.org/10.1038/s41598-020-80331-z

Lucius, M. A., Johnston, K. E., Eichler, L. W., Farrell, J. L., Moriarty, V. W., & Relyea, R. A. (2020). Using machine learning to correct for nonphotochemical quenching in high-frequency, in vivo fluorometer data. *Limnology and Oceanography: Methods*, *18*(9), 477–494. https://doi.org/10.1002/lom3.10378

Lundsør, E., Eikrem, W., Stige, L. C., Engesmo, A., Stadniczeñko, S. G., & Edvardsen, B.

(2022). Changes in phytoplankton community structure over a century in relation to environmental factors. *Journal of Plankton Research*, *44*(6), 854–871. https://doi.org/10.1093/plankt/fbac055

Mignot, A., Ferrari, R., & Claustre, H. (2018). Floats with bio-optical sensors reveal what processes trigger the North Atlantic bloom. *Nature Communications*, *9*(1), 190. https://doi.org/10.1038/s41467-017-02143-6

Mojica, K. D. A., Behrenfeld, M. J., Clay, M., & Brussaard, C. P. D. (2021). Spring Accumulation Rates in North Atlantic Phytoplankton Communities Linked to Alterations in the Balance Between Division and Loss. *Frontiers in Microbiology*, *12*(August), 1–12. https://doi.org/10.3389/fmicb.2021.706137

Roesler, C., Uitz, J., Claustre, H., Boss, E., Xing, X., Organelli, E., et al. (2017). Recommendations for obtaining unbiased chlorophyll estimates from in situ chlorophyll fluorometers: A global analysis of WET Labs ECO sensors. *Limnology and Oceanography: Methods*, *15*(6), 572–585. https://doi.org/10.1002/lom3.10185

Rumyantseva, A., Henson, S., Martin, A., Thompson, A. F., Damerell, G. M., Kaiser, J., & Heywood, K. J. (2019). Phytoplankton spring bloom initiation: The impact of atmospheric forcing and light in the temperate North Atlantic Ocean. *Progress in Oceanography*, *178*(October), 102202. https://doi.org/10.1016/j.pocean.2019.102202

Sakshaug, E., Johnsen, G. H., & Kit M. Kovacs, E. (2009). *Ecosystem Barents Sea.* (E. Sakshaug, G. H. Johnsen, & E. Kit M. Kovacs, Eds.). Tapir Academic Press,.

Scott, J. P., Crooke, S., Cetinić, I., Del Castillo, C. E., & Gentemann, C. L. (2020). Correcting non-photochemical quenching of Saildrone chlorophyll-a fluorescence for evaluation of satellite ocean color retrievals. *Optics Express*, *28*(3), 4274.

https://doi.org/10.1364/oe.382029

Slagstad, D., & McClimans, T. A. (2005). Modeling the ecosystem dynamics of the Barents sea including the marginal ice zone: I. Physical and chemical oceanography. *Journal of Marine Systems*, *58*(1–2), 1–18. https://doi.org/10.1016/j.jmarsys.2005.05.005

Son, Y.-T., Chang, K.-I., Yoon, S.-T., Rho, T., Kwak, J. H., Kang, C. K., & Kim, K.-R. (2014). A newly observed physical cause of the onset of the subsurface spring phytoplankton bloom in the southwestern East Sea/Sea of Japan. *Biogeosciences*, *11*(5), 1319–1329. https://doi.org/10.5194/bg-11-1319-2014

Sverdrup, H. U. (1953). On Conditions for the Vernal Blooming of Phytoplankton. *ICES Journal of Marine Science*, *18*(3), 287–295. https://doi.org/10.1093/icesjms/18.3.287

Williamson, D., Fragoso, G., Majaneva, S., Dallolio, A., Halvorsen, D., Hasler, O., et al. (2023). Monitoring Algal Blooms with Complementary Sensors on Multiple Spatial and Temporal Scales. *Oceanography*, 2022–2024. https://doi.org/10.5670/oceanog.2023.s1.11

Xing, X., Briggs, N., Boss, E., & Claustre, H. (2018). Improved correction for non-photochemical quenching of in situ chlorophyll fluorescence based on a synchronous irradiance profile. *Optics Express*, *26*(19), 24734. https://doi.org/10.1364/oe.26.024734

Yamaguchi, R., Rodgers, K. B., Timmermann, A., Stein, K., Schlunegger, S., Bianchi, D., et al. (2022). Trophic level decoupling drives future changes in phytoplankton bloom phenology. *Nature Climate Change*, *12*(5), 469–476. https://doi.org/10.1038/s41558-022-01353-1